COMPARISON OF HEATING PROTOCOLS FOR DETECTION OF DISBONDS IN LAP JOINTS

William P. Winfree

MS 231
NASA, Langley Research Center
Hampton, VA 23665

B. Scott Crews and P.A. Howell

Analytical Services and Materials, Inc.
MS 231
NASA, Langley Research Center
Hampton, VA 23665

INTRODUCTION

With the increased concern for the safety and reliability of aging aircraft, new nondestructive techniques are being sought for detecting and characterizing defects in these structures. These techniques must be both reliable and economical to impact the current safety of the fleet. To meet both of these requirements, more focus is being placed on large area inspection techniques. These offer the possibility for greatly reduced inspection times as compared to current point measurement techniques.

The integrity of bonded and riveted lap joints has been identified as an area where a viable technique is required for detecting disbonds. One technique which has possible application in this area is thermography. Thermographic techniques have an advantage over techniques such as ultrasonics by being noncontacting and large area measurement system. Previous research has shown that thermography is able to detect disbonds in lap joint structures [1].

The thermographic technique presented here for the detection of lap joint disbonds utilizes a radiant heat source to heat the front surface of the lap joint and an infrared imager to image its thermal response. To maximize the probability of detecting a disbond, the heating protocol was varied. Three different heating protocols were used. The first utilized a flash lamp as a heat source which gives a short high intensity heat flux. The other heating protocols used two banks of quartz lamps which heated the sample with a periodic heat flux and a pulsed heat flux. The time derivatives of these images are calculated to enhance the contrast between bonded and unbonded regions of the lap joint. To quantitatively compare the different heating protocols, contrast is defined to be a function of the moments of the histograms for the bonded regions and unbonded regions of the reduced

Review of Progress in Quantitative Nondestructive Evaluation, Vol. 11
Edited by D.O. Thompson and D.E. Chimenti, Plenum Press, New York, 1992

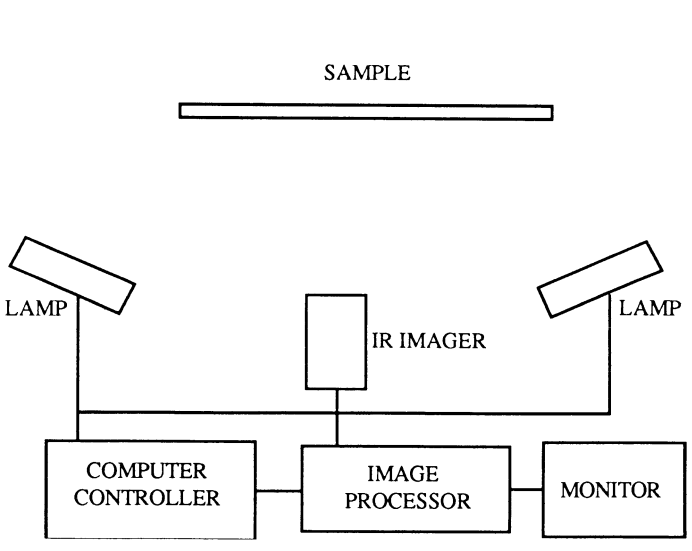

Figure 1. Schematic of experimental system.

thermal images. Comparison of the bonded-unbonded contrast for different heating times has made it possible to establish the optimum parameters to maximize the probability of detection of a disbond.

MEASUREMENT SYSTEM AND SAMPLES

A schematic of the measurement system is shown in figure 1. Two banks of lamps were used to heat the front surface of the sample. Tubular quartz lamps (4000 watts) with parabolic back reflectors focused the energy onto the sample. These imparted 0.6 watts/cm^2 to the samples of interest. The flash tubes consisted of Zenon tubes with parabolic back reflectors. They imparted 1.2 joules to the sample in less than 1/100 of a second.

An infrared imager consisting of a single liquid nitrogen cooled HgCdTe detector (8 - 12 μm) converted the infrared radiation (thermal response) from the surface of the sample to a video signal. The video output of the imager was digitized and averaged by an image processor. The averaged images were obtained for 32 different time periods. A microcomputer controlled the image processor and the application of heat. The 32 images were then transferred to the microcomputer and stored for later analysis.

The samples used, as shown in figure 2, consisted of two sheets of aluminum, bonded with a three inch overlap using a room temperature cure epoxy. The dimensions of the sheets were 61 cm by 122 cm and 0.102 cm thick. Disbonds were created by inserting pull tabs (.013 cm thick) of different dimensions into the bonded region before curing. After curing, these pull tabs were then removed to leave voids in the bond.

PHYSICAL MODEL

By heating the sample, a temperature differential is created between the lap joint regions and regions adjacent to it due to the larger heat capacity of the lap joint. A one dimensional model is used to investigate the early time history of the temperature profile. For the bonded region, the "through the thickness" time constant is dominated by the adhesive layer. For a typical epoxy adhesive, with a thermal diffusivity of 0.0010

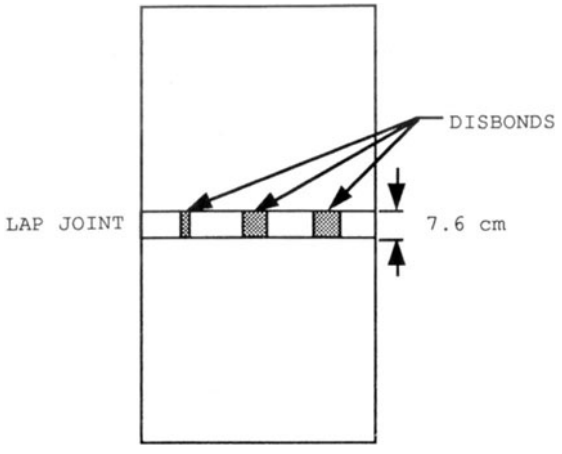

Figure 2. Typical sample configuration.

cm^2/sec and bond thickness of 0.013 cm, the "through the thickness" thermal time constant is 0.17 sec. Using the half width of a 7.6 cm lap joint of aluminum with a diffusivity of 0.86 cm^2/sec, yields a lateral thermal time constant of approximately 17 sec. Thus, the use of a one dimensional model for early times is appropriate.

For these early times, the lap joint was modeled as a three layer system with an adhesive layer bound by two other layers of identical material. Initially, the temperature of the system was assumed equal to zero and a flux is applied to the surface of one of the layers. The time dependence of the temperature was determined by numerically inverting an analytic Laplace transform solution for the system [2]. The thermal properties of the adherents and adhesives were chosen to correspond to the properties of

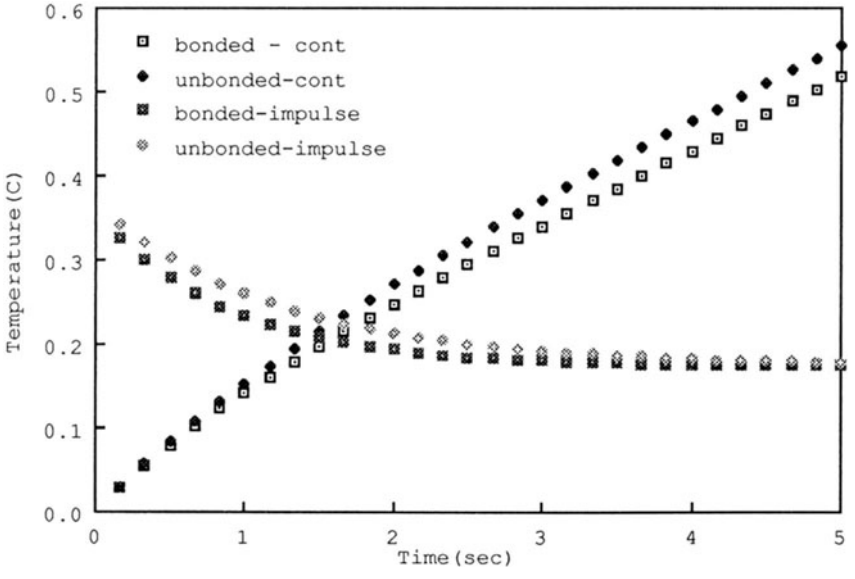

Figure 3. Thermal response of bonded and unbonded regions of lap joint to impulse and continuous heat flux.

aluminum and a typical epoxy, respectively. The thermal conductivity of the aluminum used is 0.48 cal/(sec cm ^{o}K) and for the epoxy a value of 0.00041 cal/(sec cm ^{o}K). The thicknesses of the aluminum and epoxy were chosen to be 0.101 cm and 0.013 cm.

The time dependence of the temperature of the heated surface for both impulse and continuous heating is shown in figure 3. Also shown as a comparison is the time dependence of the temperature for a disbonded system with a 10 μm air disbond. As can be seen from figure 3, the impulse heating initially gives a larger difference between the bonded and disbonded regions. As time progresses the difference between the bonded and disbonded region is greatest for the continuous heating.

These results tend to indicate that continuous heating would be the best heat source, for as time progresses the differential between bonded and unbonded increases. However, as the continuous heating progresses, the temperature difference between the bonded and the unbonded regions results in heat flowing from the unbonded to the bonded regions. This lateral heat flow reaches an equilibrium state in a period of time dependent on the shape of the disbond, with smaller disbonds obtaining an equilibrium sooner than the larger disbonds. Therefore, the optimum heating protocol depends on the size and shape of the disbond. The relationship between heating times and improved contrast are investigated with a two dimensional finite element model and is presented elsewhere [3].

DATA ANALYSIS

Previous work indicated that the time derivative of the temperature results in an increased contrast between the bonded and disbonded regions [1]. To increase the signal to noise ratio in the time derivative, a time series of images was used in the calculation. This was done by fitting the infrared images, point by point, with a second order polynomial. The time derivative was then obtained by taking the derivative of the polynomial at the center point of the time sequence. To acquire an image which was equal to the time derivative at the midpoint of the time series, the images were summed after each image in the time series is multiplied by a constant f(i,n), where f(i,n) is defined as

$$f(i,n) = \frac{12i - 6n - 6}{n^3 - n} \qquad (1)$$

where i is the number of the image and n is the total number of images in the time sequence. For this implementation, any number of images can be used and the number sequence must start with one for the first image. For the periodic and pulse heating, the 32 images were divided into two time series, the first 16 and last 16 corresponding to heat application and post heat application, respectively. For the flash heating, the last 29 images of the sequence were used.

The resulting images were viewed to determine the area of the disbond which could be resolved. To facilitate the analysis of the images, histograms were taken for the different regions on the images corresponding to bonded, disbonded and single thickness aluminum. The overlap between the histograms for these regions was a measure of the ability of the technique to detect disbonds of a given size. Therefore, a comparison of the histograms for different heating times and of the time derivatives at different points in the time series was useful for establishing the optimum heating protocol and data reduction technique for each disbond size.

To further facilitate comparison of these histograms, a moment analysis

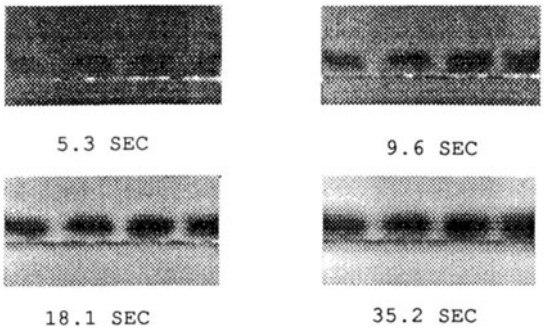

Figure 4. Time derivatives of IR images from cyclic heating of sample shown in figure 2. Period for heating cycle given under each image.

of the histograms was performed. The first three moments of the histogram are defined as

$$M_0 = \sum_{i=1}^{m} c_i \qquad (2),$$

$$M_1 = \sum_{i=1}^{m} i c_i \qquad (3),$$

and

$$M_2 = \sum_{i=1}^{m} i^2 c_i \qquad (4),$$

where m is the number of channels in the histogram and c_i is the number of counts per channel. For a gaussian distribution M_1/M_0 is the location of the peak of the distribution and the half width at half maximum (w) is given by

$$w = 1.17\left(\frac{M_2}{M_1} - \left(\frac{M_1}{M_0}\right)^2\right)^{1/2} \qquad (5).$$

A comparison of the widths of the histograms to the separation of the peaks for the different regions of the image indicates the contrast between the different regions. For this work the contrast between the bonded and unbonded regions is defined as

$$\text{contrast} = 2\frac{|p_u - p_b|}{w_u + w_b} \qquad (6),$$

where p_u and p_b are the peaks of the histograms of the unbonded and bonded regions, respectively, as approximated from equation (4) and w_u and w_b are the widths of the histograms of the unbonded and bonded regions, respectively, as approximated from equation (5). The contrast between bonded and unbonded regions was determined for each time derivative image.

RESULTS AND DISCUSSION

The time derivative images for four different period heating times are shown in figure 4. These were obtained from infrared images obtained using the sample shown in figure 2. All of the disbonds, the smallest being 2.5

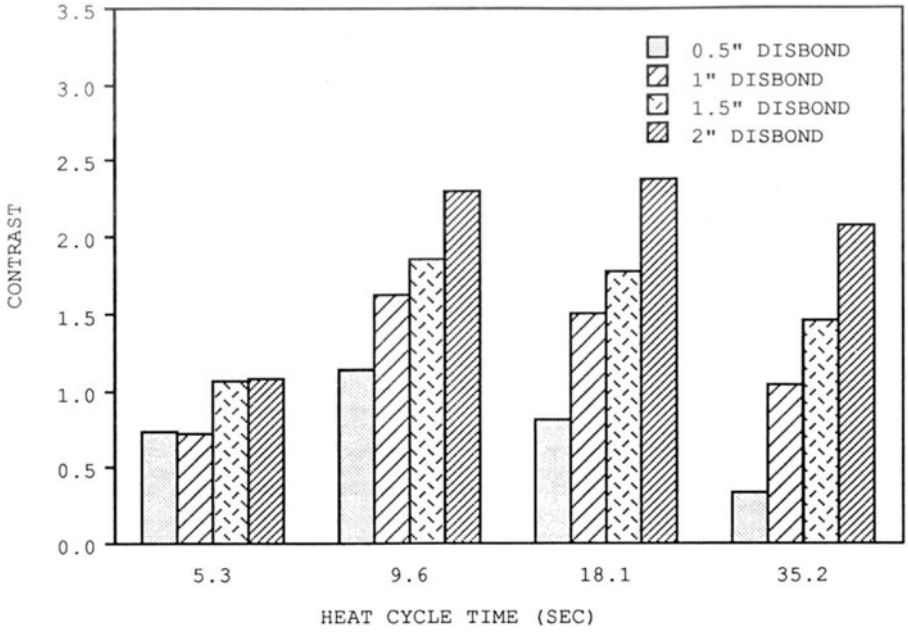

Figure 5. Contrast as a function of period time and disbond width for periodic heating.

cm wide, are clearly discernible in these images. The visual inspection of these images suggest that the contrast between the disbonded and bonded regions is greater for the 9.6 and 18.1 second heating cycles than for the 5.3 and 35.2 second cycles. Comparison of 9.6 and 18.1 second periods by visual inspection suggests that the contrast for the largest disbond continues to increase. However, for the 2.5 cm disbond it is questionable if the contrast is improving or degrading. This emphasizes the need for a quantitative characterization of contrast.

A quantitative comparison of these images is possible by calculating the contrast between the bonded and unbonded regions of the time derivative images. Results are shown in figures 5, 6 and 7 for the three different heating protocols during the cool down. These represent the average values for computed contrast for 5 different measurements on three different samples. The computed contrast for the periodic heating, shown in figure 5, has approximately the same trends as the visual perception of contrast in the images in figure 4. One possible feature that can be determined from this figure is that the contrast for the 2.5 cm disbond slightly decreases between the 9.6 and 18.1 second periods.

Comparing the contrast for different disbond sizes indicates the optimum measurement time depends on the size of the disbond change as expected. For example the optimum period for heating for the 1.3 cm disbond is clearly 9.6 seconds, while the optimum heating time for the 5.1 cm disbonded is 18.1 seconds. This effect is independent of the type of heating protocol used, therefore is a result of the geometry of the disbond.

Finally a comparison of the different heating protocols indicates for the disbonds 2.5 cm and larger the contrast is always greatest using the periodic or pulsed heating. For the smallest disbond, the impulse heating appears to give the greatest contrast. This is intuitively understandable, since the smaller the disbond, the shorter the desired time of the heating. This will effectively reduce the amount of time for lateral heat flow.

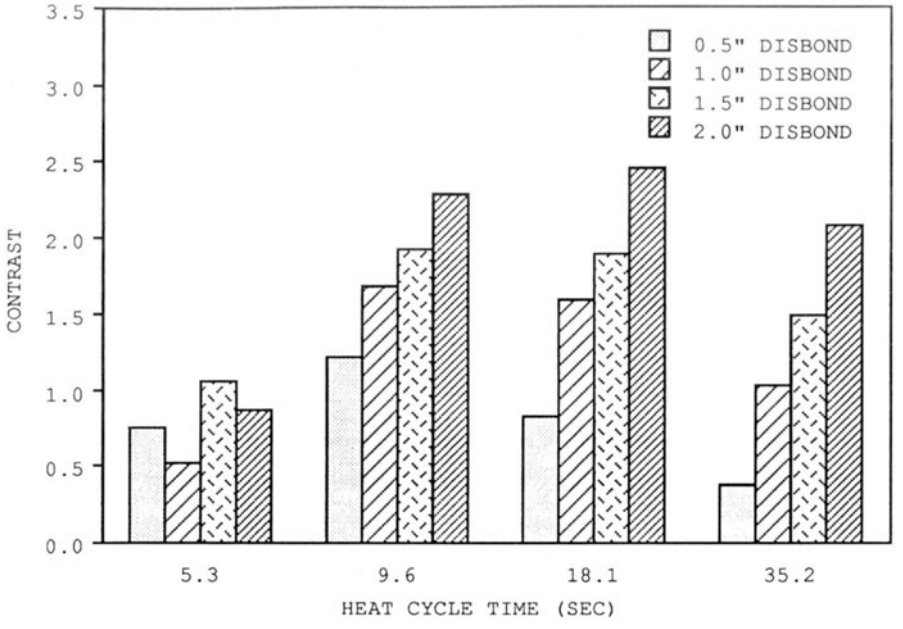

Figure 6. Contrast as a function of acquisition time and disbond width for pulse heating.

It should also be noted that there is very little difference between the results for the pulsed heating and cyclic heating. This indicates that for these structures there is little advantage gained by allowing the sample to cool longer than the cool down inherent in the cyclic heating protocol. The cyclic heating, however, is very advantageous since the period of time for acquisition of the data is significantly less.

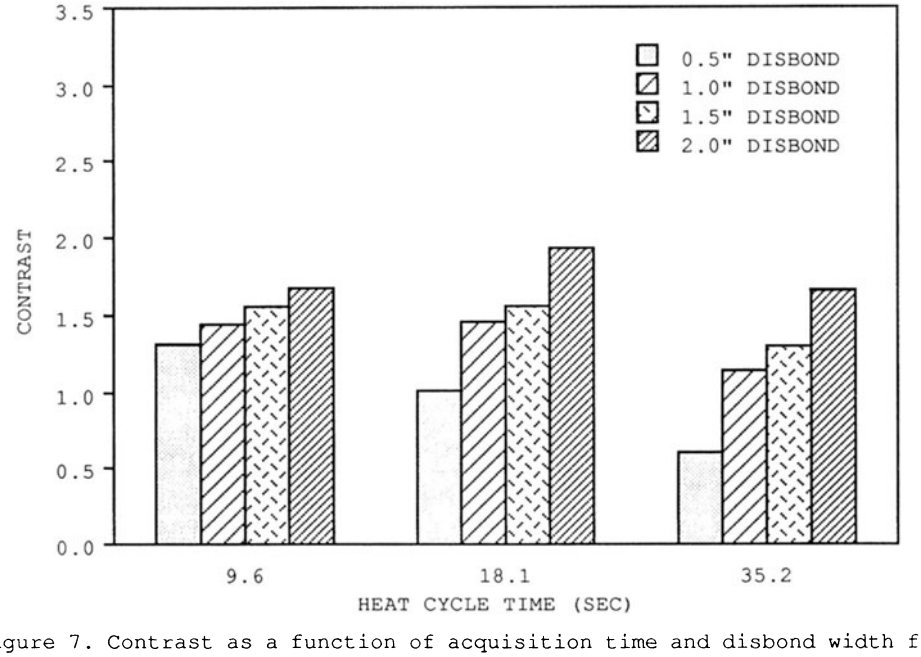

Figure 7. Contrast as a function of acquisition time and disbond width for impulse heating.

CONCLUSION

A thermographic technique has been shown to be effective for the detection of disbonds in lap joint samples. Different heating protocols show that the shorter heating times allow for the greatest contrast in smaller disbonds. The optimum heating technique for this case is periodic heating. One consideration for future study is a determination of the optimum technique for reducing the data. For the purposes of comparison, the data reduction for these types of heating are the same. Better contrast can be obtained for any of the techniques by adapting the data reduction scheme to the form of the heating protocol.

REFERENCES

1. W.P. Winfree, B.S. Crews, H. Syed, P. Howell, and K.E. Cramer, Proceedings of the 37th International Instrumentation Symposium, pp 1097-1105, (1991).

2. H.S. Carslaw and J.C. Jaeger, Conduction of Heat in Solids, Second Edition, Clarenton Press, Oxford, 1986.

3. P.A. Howell and W.P. Winfree, and B.S. Crews, Review of Progress in Quantitative Nondestructive Evaluation, 10B, pp 1367-1374 (1991).